Fundamentals of the Wet-Process Phosphoric Acid Production. 1. Kinetics and Mechanism of the Phosphate Rock Dissolution

ARTICLE *in* INDUSTRIAL & ENGINEERING CHEMISTRY RESEARCH · NOVEMBER 1996

Impact Factor: 2.59 · DOI: 10.1021/ie960092u

1 AUTHOR:

Sergey V. Dorozhkin
N/A

179 PUBLICATIONS **4,007** CITATIONS

SEE PROFILE

Fundamentals of the Wet-Process Phosphoric Acid Production. 1. Kinetics and Mechanism of the Phosphate Rock Dissolution

Sergey V. Dorozhkin[†,‡]

Research Institute of Fertilizers and Insectofungicides, Moscow, Russia

This paper is devoted to the fundamentals of natural phosphate rock dissolution under conditions close to those in the industry of the wet-process phosphoric acid production. The dissolution kinetics and mechanism of single crystals of natural fluorapatite at micro- and nanolevels have been studied for the first time. Methods of optical and scanning electron microscopy and Auger electron and IR reflection spectroscopy were used for the investigations. As a result, effects of dislocation acceleration of dissolution rate (increasing to 1.6 times) and random fluctuations of crystal size with parameter 1.15 ± 0.05 μm were discovered. Both phenomena have been described as a micromechanism of dissolution. A new system of five chemical equations for the acidic dissolution of fluorapatite has also been proposed and described as a nanomechanism of dissolution. The obtained results are useful for elaboration of new technological and ecological principles of wet-process phosphoric acid production.

1. Introduction

The wet-process phosphoric acid (WPPA) is the main intermediate for phosphorus fertilizer production (Becker, 1989; Slack, 1967; Noyes, 1967). Now a total capacity of all the WPPA-producing plants is about 26−28 million tons of P_2O_5/yr (*Phosphorus Potasssium*, 1991). So, a large number of scientific investigations on fundamentals and engineering problems of the WPPA production has already been made. Some of them are mentioned in the reference list.

However, the process of phosphate rock dissolution occurring inside an industrial reactor is not quite clear yet. It becomes obvious after an analysis of recently published papers (Beskov et al., 1991; Kafarov et al., 1991, 1990; Van der Sluis et al., 1987; Blose et al., 1984; Grinevich et al., 1983). All of them are devoted mainly to mass-transfer problems and are based upon fundamentals obtained earlier by other scientists (Chepelevetskii et al., 1937; 1956; Brutskus and Chepelevetskii, 1950; Huffman et al., 1957; Lovell, 1958; Janikowski et al., 1964). On the other hand, from the 1970s a goal of some investigations was changed to ecological problems. The investigators looked for better industrial conditions (i.e., the optimal temperature, concentration of reagents, correlation between liquid (WPPA) and solid (phosphate rock) phases, agitation intensity, etc.) for new kinds of natural phosphate rock (Elnashaie et al., 1990; Calmanovici and Guilietti, 1990; Petropavlovskii and Bespalov, 1988; Ishaque et al., 1983). These investigators have succeeded in improving the situation for 1−2 WPPA-producing plants using only this new kind of phosphate rock (e.g., increasing a total output by 0.5−1%), but the modern ecological attitude requires qualitative changes in the fertilizer industry.

Great progress achieved in raising the exactness of measurement equipment has made it possible to get additional information on fundamentals of the WPPA production. So the goal of this paper is to give a new answer for the old question: "How do crystals of the natural phosphate rock dissolve in phosphoric acid solution under conditions of WPPA production?" Contrary to the above-mentioned authors, who studied the dissolution process simultaneously for thousands of crystals in bulk, here special attention is paid to the dissolution of single crystals of the natural phosphate rock. As a result, new scientific information has been obtained. This information can lead to new engineering ideas for creation of ecological principles for the WPPA production industry. However, any problems of $CaSO_4 \cdot xH_2O$ (where $x = 2, 0.5, 0$) epitaxial crystallization and coatings formation on a surface of phosphate rock crystals are not considered here. They will be discussed later.

2. Experimental Section

Single crystals of the natural Khibin (Kola) fluorapatite (FAP) have been chosen for our experimental investigations. The choice of the phosphate rock has been made for the following reasons: (1) Khibin (Kola) FAP is a magmatic kind of natural phosphate rock with good crystallized single crystals. (2) Its chemical composition is very close to $Ca_{10}(PO_4)_6F_2$. (3) The FAP crystals can be easily distinguished and separated from crystals of other admixture minerals by an optical microscope and a needle. (4) Khibin (Kola) rock is the most popular kind of natural phosphate rock for the fertilizer industry in the former USSR. From a scientific standpoint, the natural FAP is a good object for studying a process of complex treatment for a mineral raw material.

All the experimental investigations can be divided into two main groups. The first one dealt with the dissolution process of single FAP crystals in a stream of phosphoric acid solution. The experimental conditions were as follows: pure phosphoric acid, 0−16 M H_3PO_4 without any additives and a 7.2 M H_3PO_4 solution with additivies of CaO (0−4.5%) or H_2SiF_6 (0−6%). All reagents were of "pure grade" quality (<0.01% of total impurities). Temperature: 60−90 °C. Velocity of the acid stream: 0−10 mm/s (*Re* hydrodynamics: 0−100). Initial crystal size: 50−2000 μm. Correlation between masses of acid solution and FAP crystals > 10^5: 1.

A special flow installation has been constructed for the investigations (Figure 1). One or several FAP crystals (4) were placed on a special thermostatic holder (6) with the shape of a shallow spoon. Then the holder

† Present address: Kudrinskaja sq. 1-155, 123242 Moscow D-242, Russia.

‡ Temporary address (to be used before June 1997 for all purposes): INSERM U. 424, 11 rue Humann, 67085 Strasbourg Cedex, France. Phone: (33) 88 24 34 28. Fax: (33) 88 24 33 99. E-mail: sergey@odont3.u-strasbg.fr.

S0888-5885(96)00092-9 CCC: $12.00

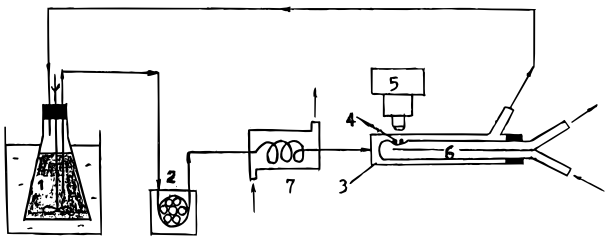

Figure 1. Experimental flow installation: 1, thermostatic flask with acid solution; 2, peristaltic pump; 3, dish from optical quartz; 4, FAP crystal(s); 5, optical microscopy with a photographic adapter; 6, thermostatic holder; 7, heater.

with FAP crystals was placed in a stream of phosphoric acid. The chemical composition of the flowing solution remained constant by using a large quantity (about 1 kg) of the acid solution in a flask (1) and a small weight (about 1 mg) of dissolving FAP crystals (4). Any changes of the crystal shape and size during their dissolution were observed and filmed by means of the optical microscope MIN-8 (5), provided with the photographic adapter MFNE-1U4.2 (both made by LOMO, Russia). The main merit of this installation is the possibility to observe and film the dissolution process for each single crystal, but it is limited by the microscope magnification (up to 100 times) and stream rates of the acid ($Re < 100$). When $Re > 100$, the nonfixed FAP crystals are usually washed away from the holder (especially on the final phases of the dissolution process).

The second group of experiments was made with a scanning electron microscope (SEM) with greater magnification. It dealt with the dissolution process of local fragments of a single FAP crystal in the pure phosphoric acid solution. A special technique has been developed for this purpose (Dorozhkin et al., 1992).

A large FAP crystal (1−2 mm) having been glued directly onto a microscope stub was dipped into a glass with the acid for a fixed period of time (usually 2−5 s). Then the stub with the crystal was quickly transferred into acetone to stop the dissolution process and to remove traces of the acid. The washing procedure is very important. The duration and composition of the washing solution determine the quality of an image obtained by the SEM. Optimum values were found experimentally, and for acetone the washing time was 15−20 s. With the shorter washing times the FAP crystals were always covered with products of the chemical interaction. Image quality was also reduced with the longer washing times. The acid could also be rinsed off by water, but in this case the optimal washing time should be decreased to 2−3 s.

After washing, the stub with the crystal was dried in air at room temperature. Then the crystal was studied and filmed by the JSM-35CF SEM (secondary electron mode) without the predeposition of a golden film. After being filmed, the crystal was taken out of the SEM and additional treatment in the acid followed. After a number of repetitions of this procedure, a series of micrographs were obtained. Comparison of these pictures has made it possible to follow the change of the same area of a single crystal during its dissolution (Figure 2). The image quality in this case was found to be as good as one obtained with vacuum predeposition of a golden film (Dorozhkin et al., 1992).

The etching process of natural FAP crystals was found to begin immediately. All the pits began to occur after 3−5 s of chemical interaction between FAP and acid solution (Figure 2a). At first their sizes were small (Figure 2a), but then they grew permanently until they covered all the crystal surface (Figure 2b−d). Their number was found not to change during dissolution. In other words, there is an equal pits number on parts a and d of Figure 2. This fact points to a dislocation structure of the crystals (Heimann, 1975; Sangwal, 1987).

Besides the SEM, methods of the IR reflection spectroscopy with Specord 70 and the Auger electron spectroscopy with Jump 10 were also used in the second group of experiments. We used standard measurement techniques for both methods and the above-described methods for crystal preparation, but a large (10 mm) previously polished natural crystal of FAP was used for the investigations.

3. Kinetics and Micromechanism of Dissolution

The experiments with the flow installation have resulted in a series of successive photographs for each dissolving single crystal. A comparison of these photographs with each other has enabled us to follow the change of their size and shape. To aid the following calculations, all the successive photographs have been printed on one sheet of a photopaper (Figure 3). Here the distances between adjacent contours divided by the time interval correspond to the rate values of the crystal dissolution in the selected direction for the selected time interval, G_{local} (m/s). The average of G_{local} values for all directions during the selected time interval is an average linear dissolution rate during this time interval, G_{time} (m/s). The average of G_{time} values for all time intervals gives an average linear dissolution rate for a whole single crystal, G_{cr} (m/s). The last value is easy to transform to the well-known value of an average mass dissolution rate from a surface unit, G_{mass} (kg/m^2 s):

$$G_{mass} = \rho_a G_{cr} \tag{1}$$

Here, $\rho_a = 3200$ kg/m^3 is FAP density.

Here, the G_{cr} value was calculated from 12 different values of G_{local} averaged according to Figure 3. After passing industrial mills, the FAP crystals always get a spontaneous irregular shape. So the largest crystal size ($\varphi = 0$ in Figure 3) was chosen as the initial one. The other 11 directions differ by 30° from each other. The following comparison has shown that 12 directions are sufficient enough for the calculations of G_{cr} values. For example, by using 24 directions the exactness of G_{cr} values increases only by ±1%.

We have found out that the FAP crystals always dissolve beginning from their surface without any disintegration (Figure 3), but different local parts of the FAP crystal surface (about 1−5 μm) dissolve with different local rates. The distribution of G_{local} is close to a Gauss distribution with one maximum. So the dissolution process can be described just by values of the average dissolution rate and its fluctuation coefficient (Melikhov et al., 1990). Cases of crystal cleavage were extremely rare during dissolution and occurred only when the initial crystals had internal cracks before. Contrary to the investigators before, who used values of the digestion coefficient (Becker, 1989; Slack, 1967; Noyes, 1967 and references therein), we were the first who applied the values of face dissolution rates G_{local} and G_{cr} as the main characteristics of the dissolution process.

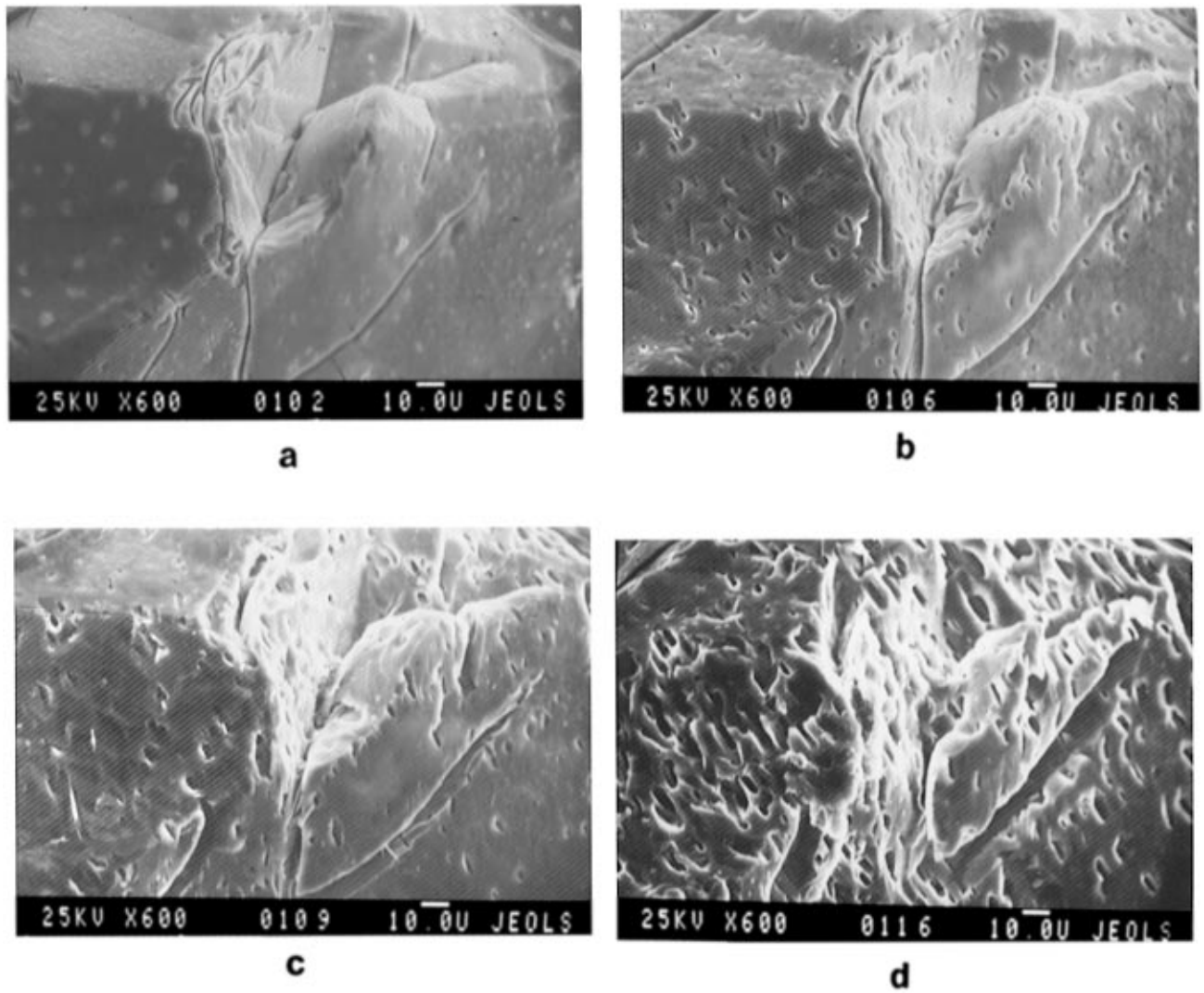

Figure 2. Example of FAP crystal dissolution, studied by the SEM (one and the same surface). Experimental conditions: 7.2 mol/dm^3 H_3PO_4, $t = 80$ °C, $Re \approx 3 \times 10^3$ (hydrodynamics), initial crystal size 1000 μm. Dissolution time: (a) 10, (b) 25, (c) 40, (d) 75 s. Bar = 10 μm.

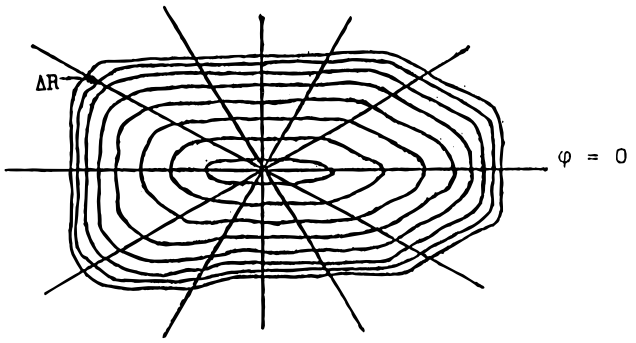

Figure 3. Dissolution scheme for a single natural FAP crystal under equal time intervals.

Sometimes among irregular FAP crystals it is possible to find regular ones. Their comparison with the habit of an ideal FAP crystal (Frye, 1981) resulted in the determination of dissolution rates for main FAP crystal faces. Dissolution rates for prism and pinacoid faces were found to be similar and approximately 1.5 times lower than those for pyramidal faces. This phenomenon has been explained by differences of etching mechanisms (Figure 4). It is well-known that usually different etching processes take place for different crystallographic faces of FAP crystals (Tyler, 1970; Jongebloed et al., 1973; Dorozhkin and Rudin, 1992). Parameters for the pits being formed on different crystal faces of the FAP are presented in Table 1.

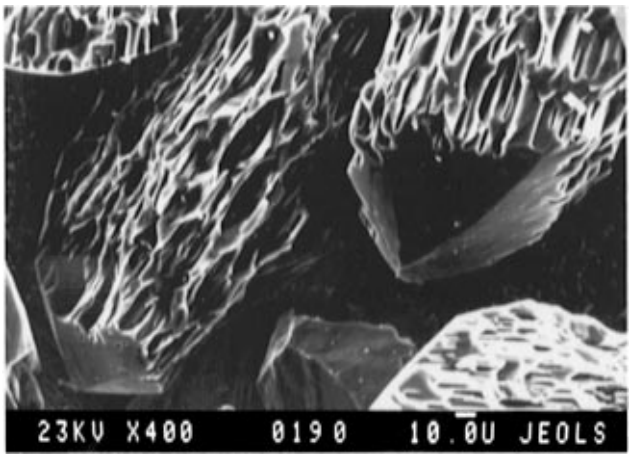

Figure 4. Differences of etching mechanisms between prism (upper right-hand corner) and pyramid (dark area just below that previously described) crystal faces of the natural FAP. Bar = 10 μm.

Moreover, crystals of the natural FAP always dissolve in acids with continuously increasing rates for all crystal faces (Figure 3). This is indicated by the increase of the distances ΔR between the adjacent contours during

Table 1. Parameters of the Etch Pits for Different Faces of the Natural FAP Crystals

type of crystal face	dimensions, μm: length	dimensions, μm: width	no. of pits/cm^2 of FAP surface	no. of tested crystals
prism	8−12	2−5	(5−8) × 10^5	>100
pyramid	5−20	2−10	100−1000	about 30
pinacoid	5−15	5−15	10^4−10^6	<100

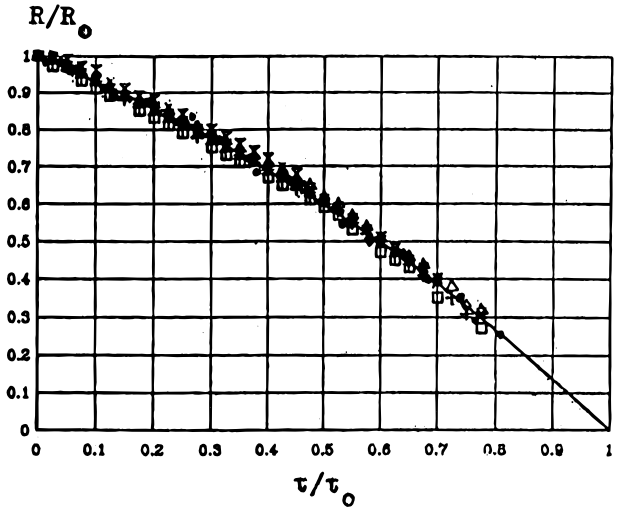

Figure 5. Change in the relative crystal size (R/R_0) during the relative dissolution time (τ/τ_0) for the natural FAP crystals. Here, R_0 and τ_0 are the initial crystal size and the full dissolution time, respectively.

equal time intervals. The change of the relative size of FAP crystals (R/R_0) versus relative time (τ/τ_0) is shown in Figure 5. To the end of the dissolution, the G_{time} value was found to increase to 1.6 times (Melikhov et al., 1990).

The experimental results have also showed that the dissolution rates G_{local}, G_{time}, and G_{cr} depend neither on the velocity of the acid flow around the crystals (in a range of 0−10 mm/s) nor on the initial crystal size. The effect of dissolution acceleration according to Figure 5 was always observed regardless of the dissolving conditions. Consequently, the discovered acceleration effect is a property of FAP crystals themselves.

To find the explanation for the acceleration effect, we used SEM. The well-known (Lovell, 1957; Tyler, 1970; Jongebloed et al., 1973) etch pits were found on the FAP crystal surface. The process of growing for several etch pits during FAP crystal dissolution was studied by the use of our technique (Dorozhkin et al., 1992). A number of pits on the FAP crystal surface were found unchanged during the dissolution (Figure 2). The pits have generally a regular faceting and a hexagonal shape according to the crystal structure of FAP (Figure 6). The pits are increased in all directions at nonuniform rates (Figure 6c) until they cover the entire crystal surface. A dissolution rate at sites of the pits formation is always higher than the average dissolution rate of an arbitrary face, because the pits are always faceted by rapidly dissolving faces only (Heimann, 1975; Sangwal, 1987). By the above-mentioned process, we explained the discovered dissolution acceleration effect.

The maximum size L_1 (length) of the etch pits usually did not exceed 20 μm (Figure 6b). To determine the pits depth and a slope of their faces, the etched crystals were split in half and then the cleavage planes were examined in the SEM (Figure 7). The pits depth was found to be proportional to their length and width and usually

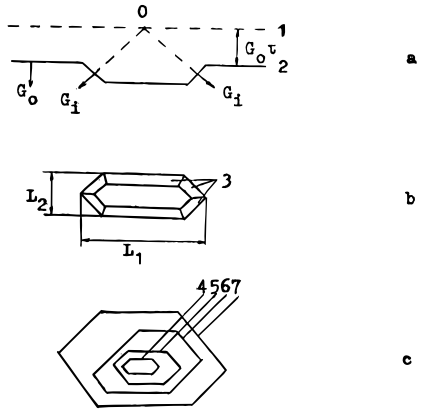

Figure 6. Development of an etch pit during the FAP dissolution: (a) profile; (b) frontal view; (c) outline of the pit at different times τ; 1, position of the dissolution front at $\tau = 0$; 2, the same at time τ; 3, sloping faces; 4−7, outlines of one and the same pit for increasing τ; 0, dislocation outcrop on the initial FAP crystal surface at $\tau = 0$.

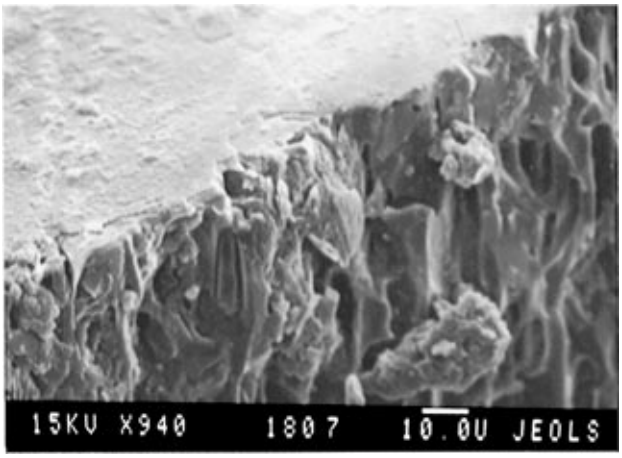

Figure 7. Fragment of the etched FAP crystal with transverse chipping for the pit's depth determination. Experimental conditions: 7.2 mol/dm^3 H_3PO_4, t = 80 °C, $Re \approx 3 \times 10^3$ (hydrodynamics), crystal size 1000 μm, dissolution time 600 s. Bar = 10 μm.

did not exceed 10−15 μm. A number of the pits were about (5−8) × 10^5 cm^{-2} on prism faces (Table 1).

The etch pits formation process is known as a result of defects (dislocations) in crystal structure (Heimann, 1975; Sangwal, 1987). For FAP crystals one etch pit corresponds to one dislocation (Lovell, 1958). So there are about (5−8) × 10^5 dislocations/1 cm^2 of prism faces of FAP crystals. A mathematical model for acidic dissolution of FAP crystals was developed on the basis of the concept of defectiveness (Melikhov et al., 1990).

The overall dissolution rate for a FAP crystal (G_{cr}) consists of the dissolution rate for local sections not occupied by the pits (G_0) and that for the sites of the pit formation (G_i):

$$G_{cr} = \frac{J}{F\rho_a} = G_0(1-\theta) + \sum_i G_i æ_i F^{-1} \qquad (2)$$

where J (kg/s) is the mass of substance reaching the solution from a crystal per unit time; F (m^2) is the projection area of the face on a plane parallel to it; ρ_a (kg/m^3) is FAP density; θ is a fraction of the projection area occupied by the pits; and $\sum_i æ_i$ (m^2) is the total surface of all sides of the pits.

Dislocations in crystals and, therefore, the formed etch pits are always distributed randomly. So, the

model for the dissolution process is based upon a Fokker−Plank equation:

$$-\frac{\partial\varphi}{\partial\tau}=\sum_i\left(f_i\frac{\partial\varphi}{\partial L_i}-D_i\frac{\partial^2\varphi}{\partial {L_i}^2}\right) \tag{3}$$

for

$$\int_0^\infty\left(f_1\varphi-D_1\frac{\partial\varphi}{\partial L_1}\right)\mathrm{d}L_2=N_0\delta(\tau) \tag{4}$$

Here, $\varphi(L_1,L_2,\tau)$ is the number of pits with length between L_1 and $(L_1 + \mathrm{d}L_1)$ and width between L_2 and $(L_2 + \mathrm{d}L_2)$ per unit area of the crystal; f_i (m/s) and D_i (m^2/s) are the rates of the directional increase in the length ($i = 1$) and in the width of the pits ($i = 2$) and their fluctuation coefficients; N_0 is the number of pits per unit of the FAP area (m^{-2}); and $\delta(\tau)$ is the Dirac function. We have

$$N_0=\int_0^\infty\mathrm{d}L_1\int_0^\infty\varphi\ \mathrm{d}L_2,\qquad \theta=\int_0^\infty L_1\ \mathrm{d}L_1\int_0^\infty\beta_0L_2\varphi\ \mathrm{d}L_2 \tag{5}$$

$$æ_i=F\int_0^\infty L_1\ \mathrm{d}L_1\int_0^\infty\beta_iL_2\varphi\ \mathrm{d}L_2 \tag{6}$$

where β_0 and β_1 are form factors describing the pits faceting.

The solution with consideration of the boundary conditions

$$\varphi(L_1,L_2,0)=\varphi(\infty,\infty,\tau)=0 \tag{7}$$

has the form

$$\varphi_i(L_i,\tau)=B_i\left[(\pi p_iA_i)^{-0.5}\exp(-{X_-}^2)-\frac{1}{2p_i}\exp\left(\frac{L_i}{p_i}\right)\mathrm{erfc}(X_+)\right] \tag{8}$$

where $B_1 = N_0$ and $B_2 = 1$, $A_i=f_{0i}\int_0^1(1-\theta)\,\mathrm{d}\tau$, $X_+ = (L_i + A_i)/2(p_iA_i)^{0.5}$, and $\mathrm{erfc}(X_+)=(2/\sqrt{\pi})\int_{X_+}^\infty e^{-X^2}\,\mathrm{d}X$. The solution has given a value of a fluctuation length $p_i = D_i/f_i = 1.15 \pm 0.05\ \mu$m. Consequently, the natural FAP crystals dissolve with microscopic fluctuations of their sizes (in other words, dissolution micromechanism for natural FAP crystals includes random irregularities equal to $1.15 \pm 0.05\ \mu$m). They should be considered when describing the dissolution process.

A complete expression for the time dependence of the linear dissolution rate has the following form (Melikhov et al., 1990):

$$G_{cr}=G_0\left[1+\left(\sum_i G_i\beta_i/G_0\beta_0-1\right)\left(\frac{1-\exp(-\tau/T)}{1+\exp(-\tau/T)}\right)^2\right] \tag{9}$$

where $T=(4{f_{01}}^2\beta_0N_0)^{-0.5}$ is a relaxation time for the surface topography of the FAP crystal. According to (9), after a time $\tau \approx 5T$, when the crystal surface is completely covered with a continuous "carpet of etch pits", the dissolution rate reaches its highest value. The obtained expression is plotted in Figure 5 and follows the experimental points quite well. Consequently, the defectiveness of natural FAP crystals causes an acceleration effect and should be considered when simulating and designing new industrial reactors for the WPPA production.

4. Nanomechanism of Dissolution

All the above-mentioned processes describe the dissolution process at the microlevel only. On the other hand, the dissolution process for FAP crystals in acids is also a chemical reaction that deals with atoms and ions. So, a nanomechanism for FAP acidic dissolution should be described too.

A process of the phosphate rock dissolution in phosphoric, sulfuric, nitric, hydrochloric, and other acids was earlier studied many times (Becker, 1989; Slack, 1967; Noyes, 1967 and references therein), but the investigators were always satisfied just with a general description of the chemical reactions as follows:

$$Ca_5(PO_4)_3F + nH_3PO_4 = 5Ca(H_2PO_4)_2 + (n-7)H_3PO_4 + HF \tag{10}$$

Reaction (10) shows that n molecules of phosphoric acid are required to dissolve one "molecule" of FAP. So, a formal application of this reaction results in a model in which each FAP crystal consists of individual "molecules" of $Ca_5(PO_4)_3F$ being attacked by some molecules of H_3PO_4 simultaneously.

Any textbook on physical chemistry mentions that an impact of more than three particles (atoms, ions, molecules, radicals) simultaneously at the same place is impossible (the possibility is extremely close to zero), but equations like (10) are usually good enough for investigators. According to our information, only Czechoslovak scientists (Jambor and Beranek, 1984) noticed this discrepancy and tried to propose a new logic of chemical interaction between FAP and acid:

$$Ca_5(PO_4)_3F + H^+ = {Ca_5(PO_4)_3}^+ + HF \tag{11}$$

$$2{Ca_5(PO_4)_3}^+ = Ca^{2+} + 3Ca_3(PO_4)_2 \tag{12}$$

$$Ca_3(PO_4)_2 + 2H^+ = Ca^{2+} + 2CaHPO_4 \tag{13}$$

$$CaHPO_4 + 2H^+ = Ca^{2+} + H_3PO_4 \tag{14}$$

As the authors noticed, this scheme consisted of bimolecular and three-molecular chemical reactions only and the three-molecular reactions (13) and (14) most probably consisted of two bimolecular reactions too. Unfortunately, the authors of this hypothesis were not able to find out any experimental arguments for its confirmation.

However, there are some results which are able to confirm the dissolution scheme (11)−(14). For example, some confirmations are mentioned in books about WPPA production (Becker, 1989; Slack, 1967; Noyes, 1967): the dissolution rate of the phosphate rock depends on H^+ concentration in a solution. This indicates the possibility of chemical reactions (11), (13), and (14). Other, indirect, confirmations were found during investigations of a defluoridization process for natural FAP crystals by water steam processing under temperatures > 1000 °C (Vol'fkovich et al., 1964) and by a mechanical wet activation in a water medium (Boldyrev et al., 1977). The last two examples hint to the possibility of chemical reaction (11), where H^+ ions can be formed by means of thermal or mechanical dissociation of water.

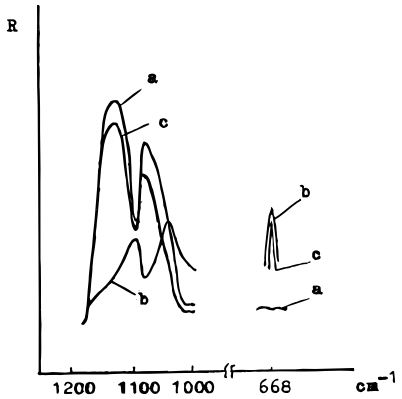

Figure 8. Comparison of infrared (IR) spectra of the diffuse reflection for (a) an initial FAP crystal surface; (b) FAP surface covered by electroconductive coating (ECC); (c) FAP surface after washing off the ECC by water.

Table 2. Wavenumbers (ν_i, cm^{-1}) of IR Spectra for the Natural FAP Crystals

	ν_1	ν_2	ν_3	ν_4	ν_5
Figure 8a	1116		1078		
Figure 8b		1100		1046	668
Figure 8c	1116		1078		668

More arguments in favor of the dissolution scheme (11)−(14) follow from results by Gusev et al. (1976) and Krivoputskaja et al. (1978). They dissolved natural FAP crystals in 0.1 N aqueous solutions of citric and hydrochloric acids under room temperature. As a result, they found the sequence of element dissolution from a FAP crystal lattice: F, then Ca, and then phosphate. Thus, they have confirmed the dissolution scheme (11)−(14).

The dissolution scheme (11)−(14) has been confirmed and even extended also by results of our own investigations. Methods of SEM, IR spectroscopy, and Auger electron spectroscopy were used for this purpose. By means of the SEM, we have found a thin electroconductive coating (ECC) being formed on FAP crystals in acids (Dorozhkin et al., 1992). It was the ECC that enabled us to make the second group of experiments mentioned above and to find out the micromechanism of dissolution. Any information about a structure and a chemical composition of the ECC enables one to find out a nanomechanism for FAP dissolution in acids. This information was obtained by the Auger electron and IR spectroscopy and by chemical analysis of the acetone used for washing.

The results obtained by IR spectroscopy are presented in Figure 8 and Table 2. They show some differences in chemical composition between the initial FAP and ECC (Figure 8a,b). After washing the ECC off with water, the chemical composition of the etched crystal surface becomes very close to that of the initial one (Figure 8a,c), but there is an essential difference between IR spectra in parts a and c of Figure 8—a new peak in the range of 668 cm^{-1}, which indicates the presence of an O−H bond (Knubovets et al., 1978). This peak characterizes vibrations for hydroxyl groups joined by a hydrogen bond to fluorine atoms in the crystal lattice of fluorohydroxyapatite. Unlike peaks of 1100 and 1046 cm^{-1}, the peak of 668 cm^{-1} was found not to be deleted by washing FAP with water. Traces of calcium and phosphate ions were discovered in water after washing out the ECC. So a water-soluble part of the ECC consists of acid calcium phosphates with an unknown exactly for the present chemical composition.

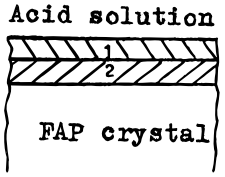

Figure 9. Structure of the surface ECC: 1, a layer of calcium acid phosphates (water-soluble part of the ECC); 2, a layer of hydroxyapatite (water-insoluble part of the ECC).

A reduction of the Ca:P molar ratio for a FAP crystal surface covered by the ECC was measured by the Auger electron spectroscopy (Dorozhkin et al., 1992). The ratio changed from 1.67 ± 0.05 (FAP) to 1.30 ± 0.05 (ECC). The obtained ratio is an intermediate value between $Ca_3(PO_4)_2$ (Ca:P = 1.5) and $CaHPO_4$ (Ca:P = 1). So, a chemical composition of the ECC is a mixture of acid calcium phosphates.

Thus, all the above-mentioned results on the assumption of a double-layer structure for the ECC are as follows: the first layer is a mixture of different acid calcium phosphates (water-soluble part), and the second layer is a solid solution of hydroxyapatite in the FAP crystal lattice (water-insoluble part). A possible scheme for the ECC is shown at Figure 9. So the dissolution scheme (11)−(14) should be completed by the following equation:

$$Ca_5(PO_4)_3F + H_3O^+ = Ca_5(PO_4)_3OH + H_2F^+ \quad (15)$$

In this case the equation (11) should be changed to:

$$Ca_5(PO_4)_3OH + H_3O^+ = Ca_5(PO_4)_3^+ + 2H_2O \quad (16)$$

As a result, the nanomechanism for FAP dissolution in acids includes irregularities of atomic (ionic) dissolutions for fluorine, calcium, and phosphate ions. The nanomechanism can be described as a system of five successive chemical equations based upon dissolution scheme (11)−(14):

$$Ca_5(PO_4)_3F + H_3O^+ = Ca_5(PO_4)_3OH + H_2F^+ \quad (17)$$

$$Ca_5(PO_4)_3OH + H_3O^+ = Ca_5(PO_4)_3^+ + 2H_2O \quad (18)$$

$$2Ca_5(PO_4)_3^+ = Ca^{2+} + 3Ca_3(PO_4)_2 \quad (19)$$

$$Ca_3(PO_4)_2 + 2H_3O^+ = Ca^{2+} + 2CaHPO_4 + 2H_2O \quad (20)$$

$$CaHPO_4 + 2H_3O^+ = Ca^{2+} + H_3PO_4 + 2H_2O \quad (21)$$

A substitution of H^+ ion in the equations (11)−(14) to its hydrate form H_3O^+ in the equations (17)−(21) is not casual here. It goes from (15), where it is the only way to describe a process of a hydroxyapatite formation on the FAP crystal surface according to the results by the IR spectroscopy.

5. Conclusions

The present investigation is an attempt to extend our knowledge about fundamentals of the natural phosphate rock dissolution under industrial conditions in the WPPA production. All the experiments were performed with crystals of natural Khibin (Kola) FAP. This might result in a question if it is possible to apply the above-mentioned conclusions to other kinds of phosphate rock.

An answer is not simple. On the one hand, all natural phosphate deposits consist of a complicated mixture of calcium phosphates (FAP, hydroxyapatite, carbonat-apatite) with other accompanying substances (mica, clay, silicates, etc.). So the nanomechanism of dissolution should be the same for any kind of phosphate rock (chemical reactions between acid and additives are not considered). On the other hand, a lot of natural phosphates do not contain as big and good single crystals as Khibin (Kola) deposit does. The crystals of other deposits are usually smaller (Becker, 1989), and this makes a complicated discovery of both the acceleration effect and microscopic fluctuations of the dissolution rate. This could be the main reason that nobody had discovered these effects earlier.

The discovered mechanism has not only a theoretical interest but also a practical significance. An industrial process of chemical beneficiation of poor natural phosphate rocks containing carbonates as admixture phases may be a good example. To increase the amount of P_2O_5, such kinds of phosphate rock are often developed by a mixture of dilute acid solution and a flotation reagent under pH = 2−4 (Becker, 1989; Slack, 1967; Noyes, 1967). Under such conditions FAP crystals are always covered by a hydroxyapatite layer that should be taken into consideration while elaborating new flotation reagents.

All new results described here do not contradict the results obtained earlier by other investigators mentioned in the reference list. The main difference between them lies in approaches to investigations. We studied fundamentals to extend knowledge at the micro- and nanolevels, while others studied close phenomena at the macrolevel.

Acknowledgment

The author expresses his profound gratitude to all editors and correctors of *Ind. Eng. Chem. Res.* for correction of his English mistakes. The author will be very glad to receive any opinions from the specialists.

List of Symbols

Latin Letters

D = fluctuation coefficient, m^2/s
f_i = rates of the directional increase in the length (i = 1) and width (i = 2) of etch pits, m/s
F = area of the face projection on a plane parallel to it, m^2
G_0 = linear dissolution rate for places not occupied by the pits, m/s
G_i = linear dissolution rate for places occupied by the pits, m/s
G_{local} = local linear dissolution rate, m/s
G_{time} = average linear dissolution rate under a time interval, m/s
G_{cr} = average linear dissolution rate for a whole crystal, m/s
G_{mass} = average mass dissolution rate from a surface unit, kg/m^2 s
J = mass of substance reaching the solution from the given face per unit time, kg/s
L_1 = length of a pit, m
L_2 = width of a pit, m
N_0 = number of pits per unit of FAP area, m^{-2}
p_i = fluctuation length, m
R = current size of a FAP crystal, m
R_0 = initial size of a FAP crystal, m
T = relaxation time of surface topography of a FAP crystal, s

Greek Letters

β_0 and β_i = form factors describing etch pits faceting
τ = current dissolution time for a FAP crystal, s
τ_0 = total dissolution time for a FAP crystal, s
ρ_a = FAP density, kg/m^3
θ = fraction of a projection area occupied by a pit
$æ_i$ = total surface of all faces of a pit, m^2
$\varphi(L_1,L_2,\tau)$ = number of pits with length between L_1 and $(L_1 + dL_1)$ and width between L_2 and $(L_2 + dL_2)$ per unit area of a crystal face at time τ
$\delta(\tau)$ = Dirac function

Literature Cited

Becker, P. *Phosphates and Phosphoric Acid*, 2nd ed.; Fertilizer Science and Technology Series; Marcel Dekker: New York, 1989; p 740.

Beskov, V. S.; Bespalov, A. V.; Kandybin, A. I.; Posokhov, V. A. Kinetics of apatite decomposition by a sulfuric acid. *Russ. J. Chem. Ind.* **1991**, *23* (No. 8), 57−60.

Blose, R.; Shakourzadeh, K.; Baratin, F. Modelisation d'un reacteur de production d'acide phosphorique. *Ind. Miner. Tech.* **1984**, *35* (No. 11), 721−726.

Boldyrev, V. V.; Kolosov, A. S.; Chajkina, M. V.; Avvakumov, E. G. Mechanochemical activation of apatite and its solubility. *Rep. Acad. Sci. USSR* **1977**, *233* (No. 5), 892−895.

Brutskus, E. B.; Chepelevetskii, M. L. Isochrons−isotherms of apatite dissolution in a H_2SO_4−H_3PO_4−H_2O system as an example of topochemical kinetics and superphosphate manufacturing. *Trans. Sci. Inst. Common Inorg. Chem. USSR, Proc. Sect. Phys.−Chem. Anal.* **1950**, *20*, 383−388.

Calmanovici, C. E.; Guilietti, M. Technological aptitude of some Brazilian phosphate rocks for acid decomposition. *Ind. Eng. Chem. Res.* **1990**, *29*, 482−488.

Chepelevetskii, M. L.; Brutskus, E. B.; Evzlina, B. B.; Krjukova, T. A.; Orlova, L. M.; Rubinova, S. S. Physico-chemical investigations of the acid treatment of phosphates. *Trans. Sci. Inst. Fert. Insectofungic., Moscow* **1937**, No. 137, 154.

Chepelevetskii, M. L.; Brutskus, E. B.; Krasnov, K. S.; Juzhnaja, E. V. Rate of minerals dissolution as a property of a multicomponent salt's systems. *Russ. J. Inorg. Chem.* **1956**, *1* (No. 7) 1512−1522.

Dorozhkin, S. V.; Rudin, V. N. Scanning electron microscopy investigations of etching Khibin apatite crystal surface in phosphoric acid solutions. *Russ. J. Chem. Ind.* **1992**, *24* (No. 2), 96−99.

Dorozhkin, S. V.; Nikolaev, A. L.; Melikhov, I. V.; Saparin, G. V.; Bliadze, V. G. Chemical preparation of dielectrics for studying their microtopography by the SEM. *Scanning* **1992**, *14* (No. 5), 112−117.

Elnashaie, S. S.; Al-Fariss, T. F.; Razik, S. M. A.; Ibrahim, H. A. Investigation of acidulation and coating of Saudi phosphate rocks. 1. Batch acidulation. *Ind. Eng. Chem. Res.* **1990**, *29*, 2389−2401.

Frye, K., Ed. *The Encyclopedia of Mineralogy*; Encyclopedia of earth science; Hutchinson Ross Publishing Co.: Stroudsburg, PA, 1981; Vol. IVB, p 794.

Grinevich, A. V.; Kochetkova, V. V.; Klassen, P. V.; Alexandrov, A. V. Study of apatite decomposition in the sulfuric−phosphoric acid solutions by a radioactive indicators method. *Russ. J. Appl. Chem.* **1983**, *54* (No. 6), 1359−1360.

Gusev, G. M.; Zanin, Ju. N.; Krivoputskaja, L. M.; Lemina, L. M.; Jusupov, T. S. Transformation of apatite's composition under conditions of weathering and leaching. *Rep. Acad. Sci. USSR* **1976**, *229* (No. 4), 971−973.

Heimann, R. B. Theorie und Technische Anwendung. *Auf*lösung *von Kristallen*; Springer-Verlag: Wien, Germany, 1975; p 272.

Huffman, E. O.; Cate, W. E.; Deming, M. E.; Elmore, K. L. Rates of solution of calcium phosphates in phosphoric acid solutions. *J. Agric. Food Chem.* **1957**, *5* (No. 4), 266−275.

Ishaque, M.; Ahmed, I.; Nassem, N. A. Study of decomposition of Jordan and Lagurban phosphate rock with nitric acid, hydrochloric acid and sulfuric acid. *Fert. News* **1983**, *28* (No. 2), 43−49.

Jambor, J.; Beranek, J. Kinetics of decomposition of Kola apatites by a nitric acid. *Chem. Prum.* **1984**, *34/59* (No. 6), 289−296.

Janikowski, S. M.; Robinson, N.; Sheldric, W. F. Insoluble phosphate losses in phosphoric acid manufacture by the wet

proses: theory and experimental techniques. Presented at the 18th Meeting of Fertilizer Society, London, Feb 1964; pp 3−41.

Jongebloed, W. L.; Molenaar, I.; Arends, J. Orientation-dependent etch pit penetration and dissolution of fluorapatite. *Caries Res.* **1973**, *7*, 154−165.

Kafarov, V. V.; Grinevich, A. V.; Kol'tsova, E. M.; Borisov, V. V.; Kochetkova, V. V.; Katunina, A. B. Mathematical modeling of decomposition process of Khibin apatite under conditions of wet-process phosphoric acid production by the hemihydrate method. *Russ. J. Appl. Chem.* **1990**, *63* (No. 11), 2463−2467.

Kafarov, V. V.; Kol'tsova, E. M.; Grinevich, A. V.; Maximenko, B. A. Mathematical modeling of wet-process phosphoric acid production by the dihydrate method in a multi-section reactor. *Russ. J. Teor. Found. Chem. Eng.* **1991**, *25* (No. 5), 686−694.

Knubovets, R. G.; Portnova, A. M.; Cherenkova, G. I. Polymeric phosphate group in a low-fluorine apatite. *Rep. Acad. Sci. USSR* **1978**, *243* (No. 5), 1280−1283.

Krivoputskaja, L. M.; Lemina, L. M.; Gusev, G. M. Transformation of structure and chemical composition of mechanically activated apatite under a leaching in various mediums. *Trans. Sib. Branch Acad. Sci. USSR, Chem. Ser.* **1978**, Issue 2, No. 4, 65−71.

Lovell, L. C. Dislocation etch pits in apatite. *Acta Metall.* **1958**, *6*, 775−778.

Melikhov, I. V.; Dorozhkin, S. V.; Nikolaev, A. L.; Kozlovskaya, E. D.; Rudin, V. N. Dislocations and the rate of dissolution of solids. *Russ. J. Phys. Chem.* **1990**, *64* (No. 12), 3242−3249.

Noyes, R. *Phosphoric Acid by the Wet Process*; Noyes Development Corp. London, 1967; p 282.

Petropavlovskii, I. A; Bespalov, A. V. Kinetics of acid dissolution of high-reactive natural phosphates. *Russ. J. Teor. Found. Chem. Eng.* **1988**, *22* (No. 3), 397−400.

Phosphorus Potassium, **1991**, No, 176, 44.

Sangwal, K. *Etching of crystals (theory, experiment, and application)*; North-Holland: Amsterdam, The Netherlands, 1987; p 497.

Slack, A. V., Ed. *Phosphoric Acid*; Fertilizer Science and Technology Series; Marcel Dekker: New York, 1967; Vols. 1−2, p 1159.

Tyler, J. E. Comparative dissolution studies of human enamel and fluorapatite. *Caries Res.* **1970**, *4*, 23−30.

Van der Sluis, S.; Meszaros, Y.; Marchee, W. G. J.; Wesselingh, H. A.; Van Rosmalen, G. M. The digestion of phosphate ore in phosphoric acid. *Ind. Eng. Chem. Res.* **1987**, *26*, 2501−2505.

Vol'fkovich, S. I.; Illarionov, V. V.; Ionass, A. A.; Malyj, A. L.; Remen, R. E. *Hydrothermal phosphorites processing to fertilizers and fodder*; Chemistry Publisher: Moscow, 1964; p 172.

Received for review February 20, 1996
Revised manuscript received July 18, 1996
Accepted July 24, 1996[⊗]

IE960092U

[⊗] Abstract published in *Advance ACS Abstracts,* October 1, 1996.